

THREE-CLUSTER NUCLEAR MOLECULES

D. N. POENARU AND B. DOBRESCU

*Horia Hulubei National Institute of Physics and Nuclear Engineering,
P.O. Box MG-6, RO-76900 Bucharest, Romania
E-mail: poenaru@ifin.nipne.ro*

W. GREINER

*Institut für Theoretische Physik der Universität, Postfach 111932,
D-60054 Frankfurt am Main, Germany
E-mail: greiner@th.physik.uni-frankfurt.de*

A three-center phenomenological model able to explain, at least from a qualitative point of view, the difference in the observed yield of a particle-accompanied fission and that of binary fission was developed. It is derived from the liquid drop model under the assumption that the aligned configuration, with the emitted particle between the light and heavy fragment is obtained by increasing continuously the separation distance, while the radii of the light fragment and of the light particle are kept constant. During the first stage of the deformation one has a two-center evolution until the neck radius becomes equal to the radius of the emitted particle. Then the three center starts developing by decreasing with the same amount the two tip distances. In such a way a second minimum, typical for a cluster molecule, appears in the deformation energy. Examples are presented for ^{240}Pu parent nucleus emitting α -particles and ^{14}C in a ternary process.

1 Introduction

Fission approach¹ to the cluster radioactivities² and α -decay has been systematically developed during the last two decades (see Ref. 1 and the references therein) as an alternative to the many-body theory.³ One has to stress the quantum nature of these decay modes and of the fission process as well. The three groups of binary phenomena are taking place by tunneling through a potential barrier. Fission theory has also been extended toward extremely large mass asymmetry⁴ to study the evaporation of light particles from a hot excited compound nucleus, going over the barrier. In a cold binary fission^{5,6,7} the fragments and the parent are neither excited nor strongly deformed, hence no neutron is evaporated; the total kinetic energy of the fragments equals the released energy.

A more complex phenomenon, the particle-accompanied fission (or ternary fission) was observed both in neutron-induced and spontaneous fission. It was discovered^{8,9} in 1946. Several such processes, in which the charged particle is a proton, deuteron, triton, $^3\text{--}^6\text{He}$, $^6\text{--}^{11}\text{Li}$, $^7\text{--}^{14}\text{Be}$, $^{10\text{--}17}\text{B}$, $^{13\text{--}18}\text{C}$,

$^{15-20}\text{N}$, $^{15-22}\text{O}$, have been detected. Many other heavier isotopes of F, Ne, Na, Mg, Al, Si, P, S, Cl, Ar, and even Ca were mentioned.¹⁰

A very powerful technique, based on the fragment identification by using triple γ coincidences in the large arrays of Ge-detectors, like GAMMASPHERE, was employed to discover new characteristics of the fission process,^{11,12} and new decay modes¹³ (emission of an alpha particle and of ^{10}Be , accompanying the cold fission of ^{252}Cf , the double fine structure, and the triple fine structure in binary and ternary fission, respectively).

The possibility of a whole family of new decay modes, *the multicluster accompanied fission*, was recently envisaged.^{14,15} Besides the fission into two or three fragments, a heavy or superheavy nucleus spontaneously breaks into four, five or six nuclei of which two are asymmetric or symmetric heavy fragments and the others are light clusters, e.g. α -particles, ^{10}Be , ^{14}C , ^{20}O , or combinations of them. Examples were presented for the two-, three- and four cluster accompanied cold fission of ^{252}Cf and ^{262}Rf , in which the emitted clusters are: 2α , $\alpha+^6\text{He}$, $\alpha+^{10}\text{Be}$, $\alpha+^{14}\text{C}$, 3α , $\alpha+^6\text{He}+^{10}\text{Be}$, $2\alpha+^6\text{He}$, $2\alpha+^8\text{Be}$, $2\alpha+^{14}\text{C}$, and 4α .

The strong shell effect corresponding to the doubly magic heavy fragment ^{132}Sn was emphasized. From the analysis of different configurations of fragments in touch, we concluded that the most favorable mechanism of such a decay mode should be the cluster emission from an elongated neck formed between the two heavy fragments. The fact that the potential barrier height is lower, suggests that in a competition between aligned and compact configurations, the former should prevail.

This idea is further exploited in the following for ternary fission, by suggesting a formation mechanism of the touching configuration, based on a three-center phenomenological model, able to explain the difference in the observed yield of a particle-accompanied fission and that of binary fission. It is derived from the liquid drop model under the assumption that the aligned configuration, with the emitted particle between the light and heavy fragment is obtained by increasing continuously the separation distance, while the radii of the heavy fragment and of the light particle are kept constant. During the first stage of the deformation one has a two-center evolution until the neck radius becomes equal to the radius of the emitted particle. Then the three center starts developing by decreasing with the same amount the two tip distances. We shall show that in such a way a second minimum, typical for a cluster molecule, appears in the deformation energy.

2 Shape Parametrization

The basic condition to be fulfilled in the ternary decay process, ${}^AZ \rightarrow \sum_1^3 {}^{A_i}Z_i$, concerns the released energy (Q -value)

$$Q = M - \sum_1^3 m_i \quad (1)$$

which should be positive and high enough in order to assure a relatively low potential barrier height. The hadron numbers are conserved. We took^{17,18} the masses (in units of energy), entering in the above equation, from the compilation of measurements.¹⁶ We make the convention $A_1 \geq A_2 \geq A_3$.

For the first stage of the process, we adopt the shape parametrization of two intersected spheres with radii R_1 and R_2 . By placing the origin in the center of the large sphere, the surface equation can be written in a cylindrical system of coordinates as:

$$\rho_s^2 = \begin{cases} \rho_{sl}^2 = R_1^2 - z^2 & , \quad -R_1 \leq z \leq z_{s1} \\ \rho_{sr}^2 = R_2^2 - (z - R)^2 & , \quad z_{s1} \leq z \leq R + R_2 \end{cases} \quad (2)$$

in which z_{s1} is the position of the separation plane, and R is the distance between the two centers. This equation is valid as long as $R \leq R_{ov3}$ defined below. The fragment radius, R_1 , is kept constant during the deformation, and for a given separation distance, R , the radius R_1 is derived from the volume conservation and matching conditions. The final fragments and the initial

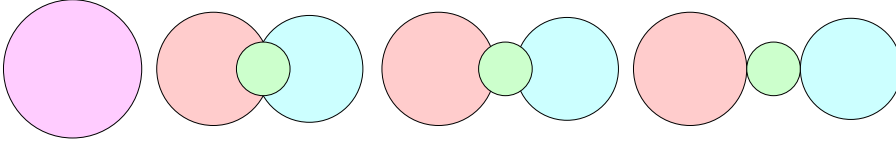


Figure 1. The assumed sequence of aligned shapes for the ternary fission of ${}^{240}\text{Pu}$, leading to ${}^{14}\text{C}$ accompanied cold fission with ${}^{132}\text{Sn}$ and ${}^{98}\text{Sr}$ fragments.

parent nucleus are assumed to possess spherical shapes with radii R_1 , R_2 , R_3 , and R_0 , where $R_j = 1.2249A_j^{1/3}$ fm ($j = 0, 1, 2, 3$). Within the range of R from $R_i = R_0 - R_1$ up to R_{ov3} one has a configuration of two overlapping spheres.

At $R = R_{ov3}$ (see the second position in Fig. 1) the neck radius $\rho_{neck1} = R_3$; R_3 is also kept constant. From that moment, the third fragment comes

into play and one has two necks and two separating planes instead of one, hence:

$$\rho_s^2 = \begin{cases} \rho_{sl}^2 = R_1^2 - z^2 & , \quad -R_1 \leq z \leq z_{s1} \\ \rho_{sc}^2 = R_3^2 - (z - z_3)^2 & , \quad z_{s1} \leq z \leq z_{s2} \\ \rho_{sr}^2 = R_2^2 - (z - R)^2 & , \quad z_{s2} \leq z \leq R + R_2 \end{cases} \quad (3)$$

In order to arrive safely at the final aligned configuration of fragments in touch with a corresponding decrease of the neck radii ρ_{neck1} and ρ_{neck2} , we assume a further elongation with a corresponding decrease of the neck radii ρ_{neck1} and ρ_{neck2} in a particular way, allowing to have the same (smaller and smaller) tip distance between the (overlapping) fragments 13 and 32 when R increases from R_{ov3} to $R_t = R_1 + R_{2f} + 2R_3$. In such a way the geometry is perfectly determined by giving one independent shape parameter, R , and the mass numbers of the parent and fragment nuclei.

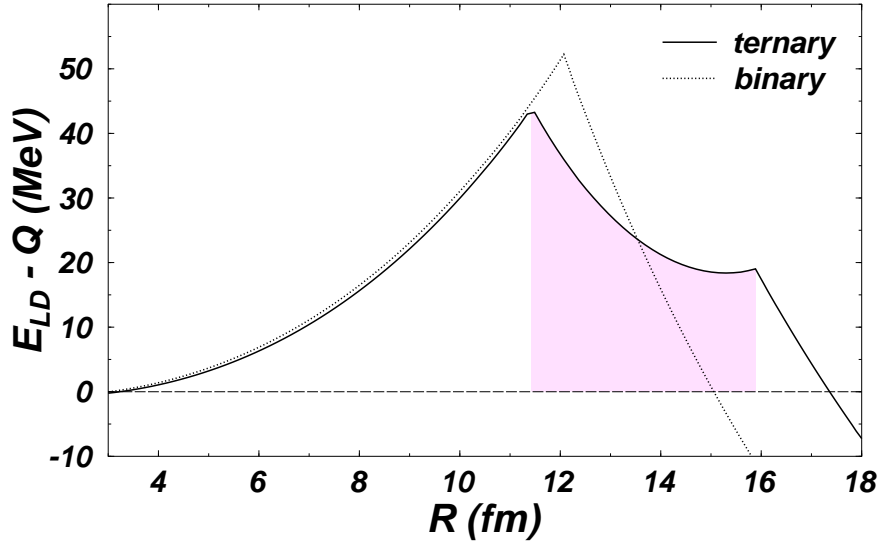


Figure 2. Deformation energy for the binary and ternary (accompanied by α emission) fission of ^{240}Pu . In both cases the heavy fragment is the double magic nucleus $^{132}_{50}\text{Sn}$. The light fragments for binary- and ternary processes are ^{108}Ru and ^{104}Mo , respectively. The region due to the development of the light particle, from R_{ov3} to R_t is emphasized.

3 Deformation Energy

According to the liquid-drop model (LDM),¹⁹ by requesting zero energy for a spherical shape, the deformation energy is defined as

$$E_{def} = (E_s - E_s^0) + (E_C - E_C^0) = E_s^0[B_s - 1 + 2X(B_C - 1)] \quad (4)$$

where $E_s^0 = a_s(1 - \kappa I^2)A^{2/3}$ and $E_C^0 = a_c Z^2 A^{-1/3}$ are energies corresponding to spherical shape. The relative surface and Coulomb energies $B_s = E_s/E_s^0$, $B_C = E_C/E_C^0$ are only functions of the nuclear shape. The dependence on the neutron and proton numbers is contained in E_s^0 and in the fissility parameter $X = E_C^0/(2E_s^0)$. The constants are $a_s = 17.9439$ MeV, $\kappa = 1.7826$, $a_c = 3e^2/(5r_0)$, $e^2 = 1.44$ MeV·fm, $r_0 = 1.2249$ fm.

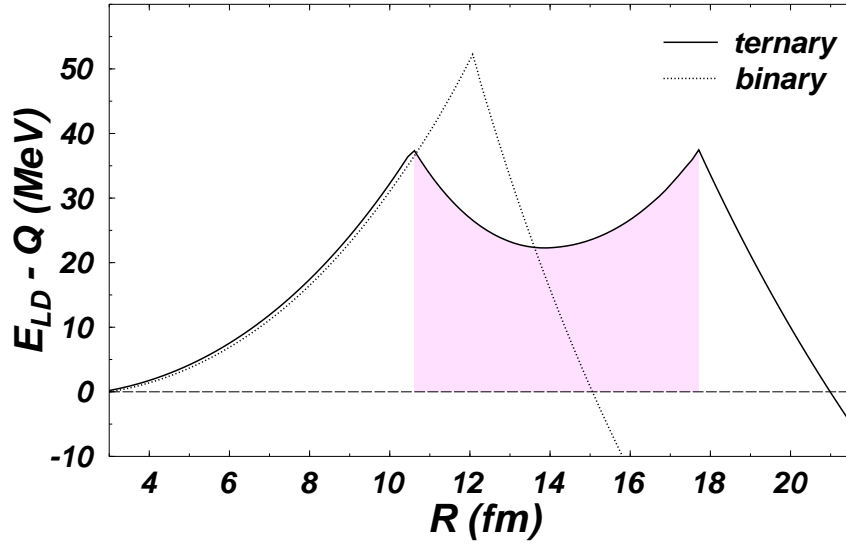


Figure 3. Deformation energy for the binary and ternary fission (accompanied by ^{14}C emission) of ^{240}Pu . In both cases the heavy fragment is the double magic nucleus $^{132}_{50}\text{Sn}_{82}$. The light fragments for binary- and ternary processes are ^{108}Ru and ^{94}Sr , respectively. The region due to the development of the light particle, from R_{ov3} to R_t is emphasized.

To the deformation energy expressed in eq. (4), we add a small phenomenological shell correction, allowing to reproduce, at $R = R_i$, exactly the

experimental Q -value in a system in which the origin of energy is taken as the sum of self energies of the fragments separated at infinity.

$$E_{LDM}(R) = E_{def}(R) + Q_{th} + (Q_{exp} - Q_{th})[1 - (R - R_i)/(R_t - R_i)] - Q_{exp} \quad (5)$$

which is $E_{def}(R) + (Q_{th} - Q_{exp})(R - R_i)/(R_t - R_i)$, where $Q_{th} = E^0 - (E_1^0 + E_2^0 + E_3^0) = E_s^0 + E_C^0 - \sum_1^3 (E_{si}^0 + E_{Ci}^0)$. In this manner the barrier height increases if $Q_{exp} < Q_{th}$ and decreases if $Q_{exp} > Q_{th}$. The correction is increased gradually with R up to R_t and then remains constant for $R > R_t$. Apart this correction, after the touching point configuration, $R \geq R_t$, one is left with the Coulomb interaction energies. For spherical fragments this has the same expression as that would be obtained for points placed into the fragment centers and carrying their whole charge.

Both the surface and Coulomb energies are calculated by performing numerical integration.^{20,21} The relative surface energy is proportional to surface area. By expressing the nuclear surface equation in cylindrical coordinates $\rho = \rho(z, \varphi)$, one has

$$B_s = \frac{1}{4\pi R_0^2} \int_{z'}^{z''} dz \int_0^{2\pi} \rho \left[1 + \left(\frac{\partial \rho}{\partial z} \right)^2 + \left(\frac{1}{\rho} \frac{\partial \rho}{\partial \varphi} \right)^2 \right]^{1/2} d\varphi \quad (6)$$

where z', z'' are the intersection points of the nuclear surface with Oz axis. Generally speaking, the Coulomb energy, E_C , for a system of three fragments with different charge densities, is defined by the following six fold integrals

$$E_C = \sum_1^3 \frac{\rho_{ie}^2}{2} \int_{V_i} d^3 r_1 \int_{V_i} \frac{d^3 r_2}{r_{12}} + \sum_{j \neq k} \rho_{je} \rho_{ke} \int_{V_j} d^3 r_1 \int_{V_k} \frac{d^3 r_2}{r_{12}} \quad (7)$$

where the first three terms belong to individual fragments and the other three represent their interaction. Here $r_{12} = |\mathbf{r}_1 - \mathbf{r}_2|$. The charge densities of the compound nucleus and of the three fragments are denoted by ρ_{0e} , ρ_{1e} , ρ_{2e} and ρ_{3e} respectively. The six-fold integral is reduced to a four-fold one of the following kind.

$$E_C = \frac{\rho_e^2}{10} \int_{z'}^{z''} dz \int_{z'}^{z''} dz_1 \int_0^{2\pi} d\varphi \int_0^{2\pi} d\varphi_1 \left(\rho^2 - \frac{z}{2} \frac{\partial \rho^2}{\partial z} \right) \left[\rho_1^2 - \rho \rho_1 \cos(\varphi - \varphi_1) + \rho \frac{\partial \rho_1}{\partial \varphi_1} \sin(\varphi - \varphi_1) + \frac{(z - z_1)}{2} \frac{\partial \rho_1^2}{\partial z_1} \right] [\rho^2 + \rho_1^2 - 2\rho \rho_1 \cos(\varphi - \varphi_1) + (z - z_1)^2]^{-1/2} \quad (8)$$

for a general shape without axial symmetry. One can get three-fold integrals for shapes possessing a symmetry axis, as for example:

$$B_{c1} = b_c \int_{-1}^{x_c} dx \int_{-1}^{x_c} dx' F(x, x') \quad (9)$$

where $b_c = 5d^5/8\pi$, $d = (z'' - z')/2R_0$, and x_c is the position of separation plane between fragments with -1, +1 intercepts on the symmetry axis (surface equation $y = y(x)$ or $y_1 = y(x')$). In the integrand

$$F(x, x') = \{yy_1[(K - 2D)/3] \cdot \left[2(y^2 + y_1^2) - (x - x')^2 + \frac{3}{2}(x - x') \left(\frac{dy_1^2}{dx'} - \frac{dy^2}{dx} \right) \right] + K \left\{ y^2 y_1^2 / 3 + \left[y^2 - \frac{x - x'}{2} \frac{dy^2}{dx} \right] \left[y_1^2 - \frac{x - x'}{2} \frac{dy_1^2}{dx'} \right] \right\} \} a_\rho^{-1} \quad (10)$$

K and K' are the complete elliptic integrals of the first and second kind, respectively:

$$K(k) = \int_0^{\pi/2} (1 - k^2 \sin^2 t)^{-1/2} dt \quad (11)$$

$$K'(k) = \int_0^{\pi/2} (1 - k^2 \sin^2 t)^{1/2} dt \quad (12)$$

and $a_\rho^2 = (y + y_1)^2 + (x - x')^2$, $k^2 = 4yy_1/a_\rho^2$, $D = (K - K')/k^2$. In our computer program the elliptic integrals are calculated by using Chebyshev polynomial approximation. For $x = x'$ the function F is not determined. In this case, after removing the indetermination, we get $F(x, x') = 4y^3/3$.

4 Results

Two examples of deformation energies are presented in Figures 2 and 3. They were obtained for the α -particle-(Fig. 2) and ^{14}C (Fig. 3) accompanied fission of ^{240}Pu , by assuming a double-magic heavy fragment $^{132}_{50}\text{Sn}_{82}$. The corresponding deformation energy for the binary cold fission of the same nucleus is also shown.

We would like to stress two striking features of these plots. Besides the first (ground state) minimum there is a *second minimum*, proving the nuclear molecule character of the aligned configuration of three fragments in touch [$(^{132}\text{Sn}, ^4\text{He}, ^{104}\text{Mo})$ and $(^{132}\text{Sn}, ^{14}\text{C}, ^{94}\text{Sr})$, respectively].

On the second hand, by comparing the surface areas under the deformation energy curve of the binary and ternary pocesses, one can see the difference explaining at least qualitatively the increased yield of the binary relative to that of the ternary cold fission.

References

1. D. N. Poenaru and W. Greiner, in *Nuclear Decay Modes*, (IOP Publishing, Bristol, 1996), Chap. 6, pp. 275–336.
2. A. Sandulescu, D. N. Poenaru and W. Greiner, *Sov. J. Part. Nucl.* **11**, 528 (1980).
3. R. Blendowske, T. Fliessbach, and H. Walliser, in Ref. 1, Chap. 7 pp. 337–349.
4. L. G. Moretto, *Nucl. Phys.* **A247**, 211 (1975).
5. C. Signarbieux *et al.*, *J. Phys. Lett. Paris* **42**, L437 (1981).
6. D. N. Poenaru, M. Ivaşcu and W. Greiner in *Particle Emission from Nuclei* Vol III (CRC Press, Boca Raton, FL, 1989) 203.
7. F. Gönnenwein in *The Nuclear Fission Process* (CRC Press, Boca Raton, FL, 1991).
8. T. San-Tsiang, R. Chastel, H. Zah-Way and L. Vignerón *C. R. Acad. Sci. Paris* **223**, 986 (1946).
9. M. Mutterer and J. P. Theobald, in Ref. 1, Chap. 12, pp. 487–522.
10. F. Gönnenwein *et al.*, *Nuovo Cimento* **110 A**, 1089 (1997).
11. J. H. Hamilton *et al.*, *J. Phys. G* **20**, L85 (1994).
12. G. M. Ter-Akopian *et al.*, *Phys. Rev. Lett.* **77**, 32 (1996).
13. A. V. Ramayya *et al.*, *Phys. Rev. C* **57**, 2370 (1998). *Phys. Rev. Lett.* **81**, 947 (1998).
14. D. N. Poenaru and W. Greiner, *J. Phys. G* **25**, L7 (1999).
15. D. N. Poenaru, W. Greiner, J. H. Hamilton, A. V. Ramayya, E. Hourany, and R. A. Gherghescu, *Phys. Rev. C* **59**, 3457 (1999).
16. G. Audi and A. H. Wapstra, *Nucl. Phys.* **A595**, 409 (1995).
17. D. N. Poenaru, W. Greiner and R. A. Gherghescu, *Atomic Data Nucl. Data Tables*, **68**, 91 (1998).
18. D. N. Poenaru and W. Greiner, in *Handbook of Nuclear Properties*, (Oxford University Press, 1996), Chap. 5, pp. 131–182.
19. W. D. Myers and W. J. Swiatecki, *Nucl. Phys.* **81**, 1 (1966).
20. K. T. R. Davies and A. J. Sierk, *J. Comput. Phys.* **18**, 311 (1975).
21. D. N. Poenaru and M. Ivaşcu, *Comput. Phys. Commun.* **16**, 85 (1978).